Article

Efficient Removal of Water Soluble Fraction of Diesel Oil by Biochar Sorption Supported by Microbiological Degradation

Zorica R. Lopičić [1,*], **Tatjana D. Šoštarić** [1], **Jelena V. Milojković** [1], **Anja V. Antanasković** [1], **Jelena S. Milić** [2], **Snežana D. Spasić** [2] **and Jelena S. Avdalović** [2]

[1] Institute for Technology of Nuclear and Other Mineral Raw Materials, 11000 Belgrade, Serbia
[2] Department of Chemistry, Institute of Chemistry, Technology and Metallurgy, University of Belgrade, 11000 Belgrade, Serbia
* Correspondence: z.lopicic@itnms.ac.rs; Tel.: +381-641168232

Abstract: The contamination of the water bodies by diesel oil (DO) and its water-soluble fraction (WSF) represents one of the most challenging tasks in the management of polluted water streams. This paper contains data related to the synthesis and characteristics of the plum stone biochar material (PmS-B), which was made from waste plum stones (PmS), along with its possible application in the sorption of the WSF of DO from contaminated water. Techniques applied in sample characterisation and comparisons were: Elemental Organic Analysis (EOA), Scanning Electron Microscopy−Energy Dispersive X-ray Spectroscopy (SEM-EDX), Fourier Transform Infrared Spectroscopy (FTIR), pH (pH_{sus}) and point of zero charge (pH_{pzc}). In order to increase the overall efficiency of the removal process, sorption and bioremediation were subsequently combined. Firstly, PmS-B was used as a sorbent of WSF, and then the remaining solution was additionally treated with a specific consortium of microorganisms. After the first treatment phase, the initial concentration of diesel WSF was reduced by more than 90%, where most of the aromatic components of DO were removed by sorption. The sorption equilibrium results were best fitted by the Sips isotherm model, where the maximum sorption capacity was found to be 40.72 mg/g. The rest of the hydrocarbon components that remained in the solution were further subjected to the biodegradation process by a consortium of microorganisms. Microbial degradation lasted 19 days and reduced the total diesel WSF concentration to 0.46 mg/L. In order to confirm the non-toxicity of the water sample after this two-stage treatment, eco-toxicity tests based on a microbial biosensor (*Aliivibrio fischeri*) were applied, confirming the high efficiency of the proposed method.

Keywords: diesel; plum stone biochar; pyrolysis; sorption; bioremediation; ecotoxicology

1. Introduction

DO represents a complex mixture of aliphatic and aromatic hydrocarbons, such as multi-branched alkanes, polycyclic alkanes, polycyclic aromatic hydrocarbons (PAH), and cycloalkyl aromatic hydrocarbons [1]. Components of DO are difficult to degrade, and their persistence, possibility of bioaccumulation and toxicity pose a serious problem that needs urgent attention [2,3]. Many methods have been created for the removal of high concentrations of insoluble, floating DO fraction; unfortunately, they are often inadequate to remove the low concentrations of dissolved DO contamination [4]. The composition and the concentration of the "water soluble fraction" (WSF) of DO depend upon several factors, e.g., DO composition, properties of the water, temperature and the preparation method [5]. The WSF consists of several toxic components such as PAHs, mono-aromatic hydrocarbons (benzene, toluene, ethylbenzene and xylenes), phenols and heterocyclic compounds and heavy metals [6]. Wastewater contaminated with DO fractions should not be directly discharged, and the application of some purification is required. For this purpose, different techniques might be used, but sorption and biological remediation are

often seen as the most environmentally and economically advantageous choices. These techniques are cost-effective, relatively simple to execute, demonstrate high removal efficiencies, require minimal energy or chemical usage, and reduce the potential for secondary contamination [5].

The development of efficient sorbents from cheap, abundant and renewable waste materials represents a possible sustainable solution for resolving DO pollution. This might promote the conversion of waste streams into useful resources using novel and sustainable methods and support the circular economy principles of reducing, reusing, and recycling waste materials [7]. Sorbents made of lignocellulosic waste biomass (LCW) originating from the food industry or agriculture hold particular significance because their application decreases the deposits of waste in landfills, diminishes greenhouse gas emissions, and offers a renewed value to the wasted products [5]. Unfortunately, direct application of raw biomass often suffers from its limited sorption capacity, low stability and associated secondary pollution generation, inducing the need for modification/conversion. The LCW properties improvement can be achieved by thermo-chemical conversion of the raw biomass; for this purpose, pyrolysis has been widely used. Pyrolysis represents thermal decomposition of the raw biomass material in a wide temperature range (starting from 300 to 900 °C) in an oxygen-free environment [8]. During the pyrolysis, the main LCW components (cellulose, hemicellulose and lignin) are thermally decomposed, generating gaseous, liquid, and solid products, whose yields depend on the properties of the raw biomass materials and the operational parameters of the pyrolysis process. Biochar (BC), a stable, carbon-rich material, created as a solid product of pyrolysis, has a characteristic surface morphology rich in specific functional groups, which makes it suitable for many purposes, including sorption (water/air/soil pollutants), catalysis (e.g., syngas upgrading, biodiesel production), soil conditioning, energy application, etc. [8–10]. In recent years, the application of BC in resolving DO contamination issues, either in the soil or water medium, has gained a lot of attention [3,4,11].

However, biological agents such as microorganisms have been successfully used in the treatment of various types of pollution, from oil hydrocarbons to heavy metal pollution, up to long-lasting polluting substances. The use of microorganisms is constantly increasing due to their enormous biodiversity, unsurpassed catabolic potential, and degradation abilities through the process of reducing pollutant mass and toxicity in soil, water, and air, also known as bioremediation; although individual microorganisms pose the ability to partially break down the components of the polluting medium, microbial communities are capable for extensive degradation [12]. Due to its efficiency, cost-effectiveness, and ecologically friendly byproducts, bioremediation has been widely proposed to remove various organic contaminants from diverse environmental matrices, especially for huge amounts of low concentrated hazard pollutions [13]. Bioremediation does the least harm to the environment and is fully in line with the principles of sustainable development.

Plum (*Prunus domestica* L.) is a fruit that plays an important role in the economic and social development of the Republic of Serbia. According to the official data [14], the average production of plums in the Republic of Serbia in 2017 was 330,582 tons, which ranks Serbia at the top of the world's plum producers. If we take into account the share of the stone mass in plum fruit mass, approximately 8–10% [15], it is easy to conclude that the stated amount of fruit officially generates more than 33,000 tons of waste material. Although the lignocellulose waste can be transformed into high-value-added products, and serve as a source of energy and chemicals [16], only a negligible amount is revalorized, and most of it is landfilled.

Considering the abovementioned, in this paper, we have produced the plum stone biochar and applied it as a renewable and efficient sorbent in the purification of the water contaminated by the WSF of DO. After this, the bioremediation technique was applied in order to increase process effectiveness. To the best of our knowledge, there are no papers published with plum stone biochar and its application in the sorption of DO, sole or in combination with any bioremediation technique. Thus, the objectives of this

work were to (1) characterize the plum stone biochar and describe the structural changes induced by thermochemical conversion; (2) investigate plum stone biochar sorption ability toward the WSF of DO; (3) evaluate the contribution of the bioremediation in the overall pollutant removal and (4) demonstrate the synergy of biochar sorption and microbiological degradation with no secondary pollution generation.

2. Materials and Methods

2.1. Sorbent/Sorbate Preparation

Waste plum stones (*Prunus domestica* L.) from the local fruit processing company "Šljivko", Šatornja, Serbia, were dried at room temperature and used for all experiments without additional washing. The sample was ground by the vibrating mill "Siebtechnik—TS250" (Siebtechnik GmbH, Mülheim, Germany) and sieved to obtain a particle size of less than 0.1 mm. Further, ground plum samples (PmS) were pyrolysed at 500 °C within an argon atmosphere (flow 100 mL/min, heating rate 10 °C/min) in a Nabertherm 1300 muffle furnace (Nabertherm, Lilienthal, Germany) for 90 min. The obtained plum stone biochar sample was labelled as PmS-B.

Diesel oil was acquired from the local commercial gasoline station (NIS Petrol, Belgrade, Serbia). WSF of the DO used in sorption experiments was prepared by dissolution of 10 mL of DO in 1 L of distilled water; the suspension was vigorously mixed in a horizontal shaker (24 h, 25 °C), after which it was left for 24 h in a glass separator funnel (for settling down the phases). For the sorption experiments, a saturated solution of WSFs gathered from the bottom of the separation bottle was used.

2.2. Sorbent Characterisation

For elemental analysis, "Vario-EL III CHNS-O Elementar Analyzer" (Elementar Analysensysteme, Langenselbold, Germany) was used in the following operating ranges: 0.03–20 mg for C; 0.03–3.0 mg for H; 0.03–2.0 mg for N and 0.03–6.0 mg for S. Oxygen content was obtained by subtracting the sum of the obtained elemental values from 100%.

The ASTM D6851-02 standard [17] was applied for the determination of the contact pH (pH_{sus}). To determine it, 0.2 g of the sample was suspended in 30 mL of distilled water and stirred for 72 h at room temperature. After that, the suspension was filtered through filter paper, and the measured pH value was defined as the contact pH_{sus}. The pH meter SensION3 (Hach, Loveland, Kolorado, CO, USA) was used to measure pH values in all experiments.

The point of zero charge (pH_{pzc}) of sorbents was evaluated by Milonjić et al. [18].

The surface morphology of the PmS-B sample was analysed by Scanning Electron Microscopy–Energy Dispersive X-ray Spectroscopy (SEM-EDX). Dried samples were previously prepared by coating with a thin layer of gold under vacuum and then observed by using a JEOL JSM-6610 LV model (JEOL Ltd., Akishima, Tokyo, Japan).

For identification of the surface functional groups, Fourier Transform Infrared Spectroscopy (Thermo Nicolet 6700 International Equipment Trading Ltd., Waltham, MA, USA) was used.

2.3. Batch Sorption Experiments

For the purpose of kinetic investigations, batch sorption experiments were performed by mixing 1.5 g of PmS-B in 100 mL of the synthetic DO solution (the initial WSF concentration was 18 mg/L). Erlenmeyer flasks (250 mL) with saturated DO solutions were placed in an orbital shaker (Heidolph Unimax 1010, Schwbach, Germany) and shaken for different time intervals (2, 5, 10, 20, 30, 60, 90 and 120 min) at 25 °C at an agitation speed of 200 rpm; the pH value of the initial solution was 6.

The sorption isotherm experiments were conducted under the same operational parameters previously described, but the initial WSF concentration varied from 2 to 18 mg/L, and the equilibrium time was set to 2 h.

After the desired contact time, phases were separated by centrifuge (4000 rpm) and the WSF (liquid phase) was sent for analysis according to the SRPS EN method [19]. Gas chromatographic analyses were carried out on the Agilent 7890A gas chromatograph (Agilent Technologies, Santa Clara, CA, USA) with a flame ionization detector (FID). Obtained data were processed using ChemStation software, version LTS 01.11 (Agilent Technologies). The results are presented as the average values obtained from three replicated experiments.

The sorbent's ability to bind the sorbate was expressed through the sorption capacity (q, mg/g) and the removal efficiency (R, %) and calculated according to the following equations:

$$q_e = (C_o - C_e)/m \cdot V \qquad (1)$$

$$R = (C_o - C_e)/C_o \cdot 100\% \qquad (2)$$

where C_e and C_o are the equilibrium and the initial concentrations (mg/L), respectively; V (L) is the volume of the solution, and m (g) represents sorbent weight.

2.4. Microorganisms

The consortium used in the biodegradation process consisted of bacterial strains MT116986.1 (*Bacillus* sp.), MT117228.1 (*Pseudomonas* sp.), MT111836.1 (*Rhodococcus* sp.) and MT081361.1 (*Pseudomonas* sp.), which were isolated from the local underground water contaminated with oil hydrocarbons [20]. A few days before the biodegradation experiment, the mentioned strains were spread onto agar plates and incubated at 28 °C. The mineral salt medium [21] with 2000 ppm diesel fuel for hydrocarbon-degrading microorganisms (HD) was used. The incubation process lasted 10 days. The microbial population from the medium was used for inoculation.

After sorption and separation of the plum stone biochar, the consortium of hydrocarbon-degrading microorganisms from the agar plates was added to the aqueous solution. Nitrogen, phosphorus and potassium sources were not added to the solution. The initial number of microorganisms was 10^8 CFU/mL. The experiment lasted 19 days on a horizontal shaker at an average temperature of 28 °C.

2.5. Eco-Toxicity Test

For estimation of eco-toxicity of polluted water before and after cleaning treatment, *Aliivibrio fischeri* NRRL B-11177 (Macherey-Nagel GmbH & Co. KG, Düren, Germany) was used according to EN ISO 11348-3 Ref 1. Freeze-dried bacteria were suspended in the reconstitution solution BioFix® Lumi-10 (Macherey-Nagel GmbH & Co. KG, Düren, Germany). The sample's pH value was adjusted at 6.5–7.5, while the concentration of NaCl was 20 g dm^{-3}. Bacteria were incubated for 15 min at 15 °C with several dilutions of the samples (50%, 25%, 12.5%, 6.25% and 3.125%). The results were expressed as a per cent of inhibition and the effective concentrations causing 50% luminescence inhibition (EC_{50} values) were calculated. All tests were performed in triplicate, and the average values are presented.

3. Results and Discussion

3.1. Sorbent Characterisation

To observe changes that took place after the thermal treatment, the characterisation of the native PmS and obtained biochar, PmS-B were performed. The results of elemental composition, investigated element ratios, pH$_{sus}$ and pH$_{pzc}$ values are presented in Table 1.

Table 1. Elemental composition of PmS and PmS-B, together with pH$_{sus}$ and pH$_{pzc}$.

	N, %	C, %	H, %	S, %	O [1], %	H/C	O/C	(O + N)/C	pH$_{sus}$	pH$_{pzc}$
PmS	1.48	48.51	6.28	0.15	43.57	0.13	0.90	0.93	4.72	4.70
PmS-B	1.62	71.78	2.91	0.00	23.70	0.04	0.33	0.35	7.09	7.01

[1] Calculated as difference from 100%.

The characteristics of the pyrolysis final product depend on feedstock composition and process parameters, especially applied temperatures. The decomposition process is followed by the release of volatile matter, and the obtained product plum stone biochar is presented with a decreased amount of H and O and with a higher C concentration [5]. As can be seen from Table 1, the content of C is higher in PmS-B obtained at 500 °C (71.78%) in comparison to the raw biomass (48.51%). The results are in accordance with Li et al. [22], who investigated biochar obtained from mulberry and cinnamon woodchips through the process of pyrolysis at 550 °C and obtained a C content of 72.40 and 75.08%, respectively. It is well known that slow pyrolysis can produce high-quality stabile biochar, which is presented with a low ratio of H/C [23]. The value of the H/C ratio is an indicator of the biochar aromaticity, and a lower value of H/C in PmS-B indicates the stabile and stronger aromatic structure [5]. The electron-rich aromatic π-system can increase existing H-bonds or it can act as a proton acceptor in sorption systems [24]. Also, the value of the O/C ratio is an indicator of hydrophilicity, as can be seen from Table 1, and this value in plum stone biochar is three times lower than in the raw sample due to the lower number of polar functional groups on the surface of PmS-B, which is in accordance with the FTIR results (later in the text). According to Yang et al. [25], in biochar generally, polar (oxygen-containing) groups are mostly distributed in meso or macropores, while oxygen-containing non-polar functional groups are mainly distributed on the surface of multilayer pores. The polarity of the carbonaceous sorbents (in this case biochar) is related to their aliphatic portion and is also important in the sorption of organic compounds [26]. The (oxygen + nitrogen/carbon) index content can be used to identify the amount of polar functional groups [27]. A higher amount of oxygen-containing functional groups raises the sorbent's overall polarity, increasing the capacity for polar and ionic organic compounds and decreasing the affinity for hydrophobic compounds [26,27]. As can be seen from Table 1, thermo-chemical conversion led to a decrease in the raw material polarity from the initial value of 0.93 to 0.35. These findings are also confirmed by FTIR analyses.

In Table 1, the results of pH_{sus} and pH_{pzc} are also given. The pH_{sus} can be considered as an indicator of the overall dominance of acidic or basic functional groups present on the surface of the solid sample. Based on the results shown in Table 1, it can be concluded that the presence of acidic functional groups is dominant in the PmS (4.72), while the surface of the PmS-B (7.09) is slightly alkaline. The increase in the pH_{sus} in PmS-B can also be explained by the increased concentration of the inorganic elements in feedstock (alkali ions and carbonates formed by Na^+, K^+, Mg^{2+} and Ca^{2+} ions), which are not lost during pyrolysis [5,28].

The points of zero charge of the samples, pH_{pzc}, represent the specific pH value of the solution at which the sum of the surface charges of the solid phase is equal to zero. This characteristic of the sorbent is particularly significant when considering the behaviour of sorbents in an aqueous solution because if the operating pH value of the suspension is lower than pH_{pzc}, the surface of the solid phase is positively charged and corresponds to the binding of anions. Based on the results presented in Table 1, the value of the zero charge of the pyrolyzed sample (PmS-B) is slightly higher compared to the starting material (PmS), which is expected due to the known phenomenon in which the process of pyrolysis breaks down hemicellulose and cellulose—the main carriers of carboxyl groups—and because there is an increase in the content of the hydroxyl groups.

The SEM micrographs presented in Figure 1 indicate that the PmS surface (Figure 1a) is rough but lacks visible pores in comparison to the surface of the PmS-B (Figure 1b), which is evidently more porous, with pores of different shapes and sizes (1–30 μm). Keeping in mind that the plum stones are rich in lignin [29], the thermochemical conversion will result in the development of a macro-porous structure of the biochar. This phenomenon can be explained by the stability of lignin at higher temperatures, which will lead to the preservation of its pore structure. Also, the elimination of volatiles at higher temperatures leads to the formation of larger pores and the merging of micropores into mesopores [30]. These findings are in accordance with the study of Antanasković et al. [31], who compared

the SEM of native peach stone and its biochar and obtained that the pyrolysis promotes highly developed porous structure with large cracks and micro/mesoporous channels.
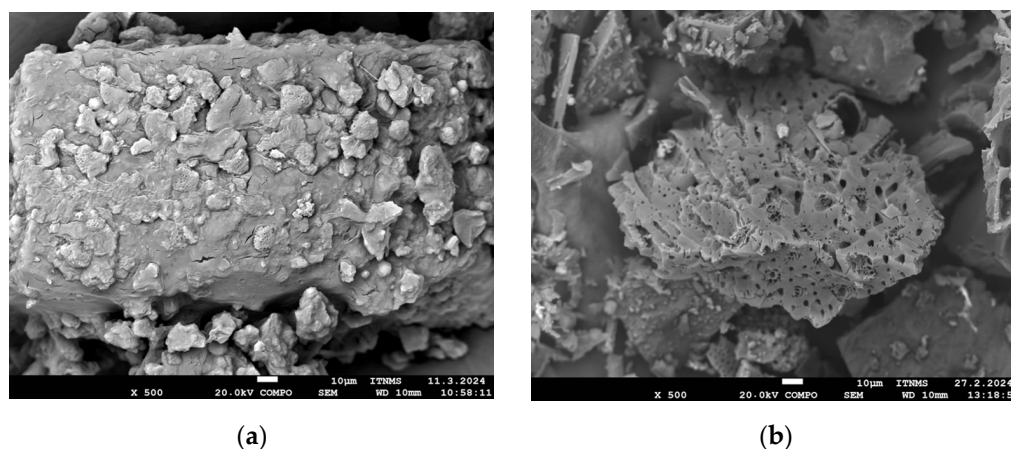

(**a**)   (**b**)

Figure 1. SEM micrograph (scale bar, 10 μm, magnification ×500) of the (**a**) PmS and (**b**) PmS-B.

EDX spectra of PmS and PmS-B, along with the detected composition, are presented in Figure S1. Gold can be observed due to the process of the sample preparation. The main proportion of the major elements confirmed the trend of EOA analysis.

To observe changes in surface functional groups that have occurred (after the process of pyrolysis and sorption of WSF), the samples were subjected to FTIR analysis, and the obtained spectra are presented in Figure 2. The FTIR spectrum of PmS showed characteristic absorption bands for lignocellulosic materials, as described in the author's previous studies [31–33]. However, after pyrolysis, the PmS-B spectrum has been significantly changed in comparison to the starting sample, as can be seen in Figure 2.
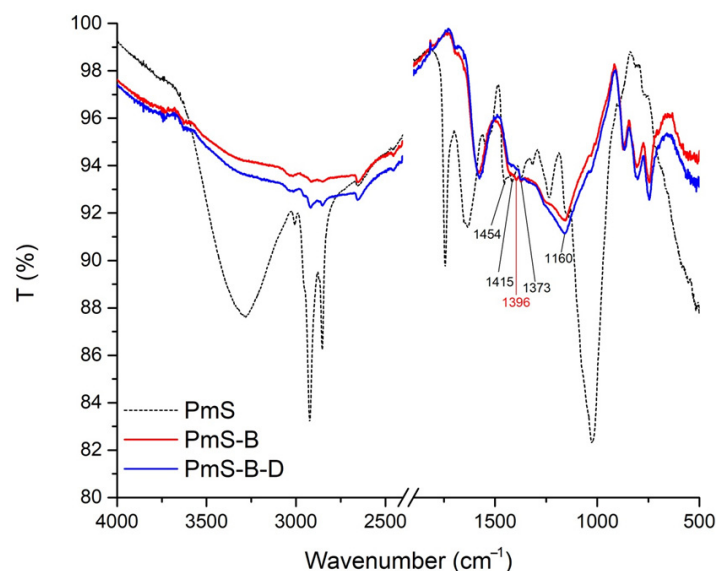

Figure 2. FTIR spectra of the plum stones (PmS), plum stone biochar (PmS-B) and plum stone biochar after sorption of the diesel fraction (PmS-B-D).

The FTIR spectrum of PmS has a typical broadband at 3282 cm^{-1} that corresponds to –OH stretching vibrations originating from alcohols, phenols and carboxylic acids and a small band observed at 3007 cm^{-1}, which can be assigned to the C=C-H stretching vibration due to the presence of fatty acids from plum kernels. Intense bands in the region 2900–2800 cm^{-1} are attributed to asymmetric and symmetric –CH$_2$ and –CH$_3$ stretching, originating from the aliphatic chains of organic acids. The sharp band at 1746 cm^{-1} is

assigned to aromatic carbonyl or carboxyl -C=O stretching of carboxylic acids or their esters, while the band at 1640 cm^{-1} is assigned to C=N [34]. The bands at 1544, 1454 and 1417 cm^{-1} are assigned to the C=C stretching in the aromatic ring [35].

After pyrolysis, some bands (3282, 2921 and 2851 cm^{-1}) decreased, while others (1746, 1454, 1417, 1317 and 1236 cm^{-1}) disappeared from the FTIR. According to Li et al. [22], the bands assigned to aliphatic CH$_2$ and CH$_3$ reduce with temperature increases up to 450 °C, indicating a reduction in the content of nonpolar groups. The disappearance of the band at 1746 cm^{-1} in PmS is related to the effect of hemicelluloses degradation, while the disappearance and reduction of bands from the fingerprint region are due to the effect of lignin depolymerisation during the process of pyrolysis [5]. For example, the disappearance of the band at 1236 cm^{-1} is attributed to C-O-C stretching from the aryl-alkyl ether linkage [36]. As we noticed in our previous paper [5] similar band shifts happened from 1544 to 1578 cm^{-1} (which is assigned to –COO$^-$ stretching) and from 1140 to 1160 cm^{-1} (assigned to asymmetric C–O–C stretching). Pronounced bands around 800 cm^{-1} originate from aromatic compounds and appear as a result of the decomposition of branched alkanes or aliphatic hydrocarbons after pyrolysis [37]. Presented FTIR spectra results showed the progression of aromatic functional groups in PmS-B compared to aliphatic groups of the PmS. This might be due to the strong volatilisation of aliphatic radicals rich in oxygen found in lignin and hemicellulose that occurs at 500 °C, where carbon chains are creating polycondensed aromatic structures [38].

After the sorption, the band at 1396 cm^{-1} was not present in the FTIR spectrum of PmS-B-D. According to Li et al. [22], this band might be assigned to the –OH bending vibration or COO– stretching vibration, and its vanishing indicates the involvement of this group in diesel sorption by plum stone biochar.

3.2. Sorption Kinetics Results

There is a variety of methods designed to describe the sorption kinetics of sorbates onto biochar sorbents, including reaction-based and diffusion-based models [39]. The first group, reaction-based models, focuses on interaction rates between the biochar and pollutants, while the diffusion-based models describe the diffusive transport of sorbate from aqueous solutions through the liquid film surrounding the sorbent particle into the sorbent pore networks (including active sites of the sorbate (biochar)). In order to investigate the mechanism of WSF sorption by PmS-B and potentially rate-controlling steps that include mass transport and chemical reaction processes, nonlinear forms of the following kinetic models were applied to the experimental data: pseudo-first-order (PFO), pseudo-second-order (PSO), the Elovich model and the Weber–Morris intraparticle diffusion model. Model equations are given in Supplementary Materials, Table S1. The correlation coefficients (R^2) between experimental data and the model equation, along with the values of chi-factor (χ^2) were used to choose the "best fit" model and distinguish between kinetic and diffusion rate control.

The kinetic profile of the WSF sorption onto the PmS-B sample is shown in Figure 3. As can be seen (Figure 3a), this sorption is very fast at the beginning; the pollutant concentration dropped from the initial 18 mg/L to 4.35 mg/L after 10 min, removing 75% of the initial concentration and accomplishing the equilibrium after 1 h, with the removal percentage of approximately 92%. The higher sorption rate during the first 30 min of the sorption was caused by the presence of free active sites on the surface of the PmS-B sample. The rapid kinetics observed for diesel removal by PmS-B facilitates smaller reactor volumes, ensuring the efficiency and economy of the practical applications of the PmS-B [40].
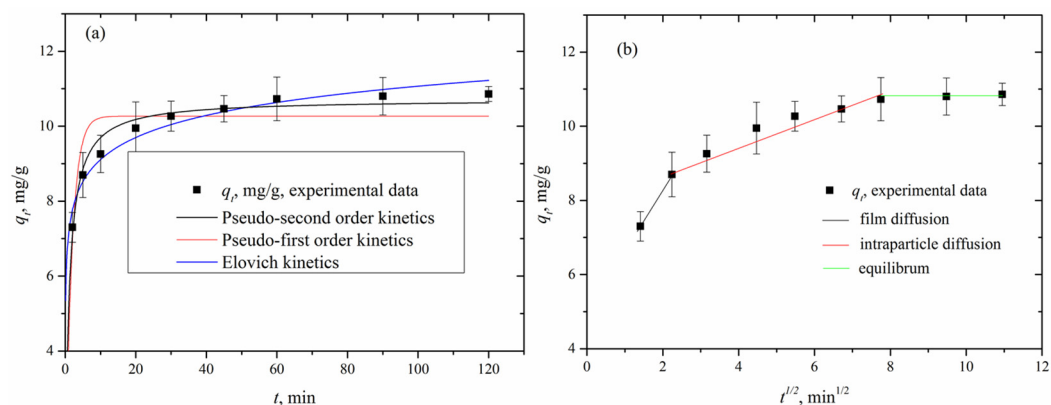
Figure 3. (**a**) Sorbed WSF per mass of PmS-B (q_t) as a function of time: experimental data (symbols) and reaction model predictions (lines), (**b**) Weber–Morris model applied on experimental kinetic data.

Experimental data were fitted by three reaction models and one diffusion model; fitting results are given in Table S2. The PFO kinetic model fits experimental data only in the first 30 min of the sorption, resulting in the lowest R^2 equal to 0.9662 and the highest value of χ^2 (0.3690). The application of the Elovich model better fitted the experimental data (Table S2), but the model equilibrium capacity value has been overestimated (11.33 mg/g) compared to the experimental value (10.80 mg/g). The correlation coefficient for the Elovich model was found to be 0.9917, while χ^2 resulted in a value of 0.0712. However, the best fit of the data was achieved by using the PSO kinetic model, where the R^2 is equal to 0.9943 and the χ^2 is the lowest, 0.0611. Furthermore, the calculated q_m value (10.72 mg/g) was the closest to the experimental q_m value. The presented results indicate that the electron sharing between WSF and PmS-B might be involved in the removal of the sorbate species, similar to our previous investigations [5]. Investigations of the diesel oil sorption by crab shell biochar [2] or sorption of the PAH compounds by biochar from the waste *Sterculia foetida* [41] have also resulted in the best fit of the experimental kinetic data by the PSO model. These studies have also shown that the diesel oil sorption (as well as its components) is closely related to the functional groups (e.g., O–H, C=O, and C–O) that are present on the sorbent surfaces. The FTIR analysis confirmed that the PmS-B sample surface is rich in these functional groups. Although the PSO model operates on the assumption that the rate-limiting step in sorption kinetics might be chemical sorption [42], it has also been found that a diffusion-controlled process is better described by PSO than by PFO [43].

It is generally accepted that the sorption dynamics consists of three consecutive steps: (i) boundary film layer diffusion that includes transport of the sorbate from the bulk solution to the sorbent external surface; (ii) intraparticle diffusion of the sorbate from the external surface into the pores of the sorbent and (iii) the final sorption of the sorbate on the active sites on the internal surface of the sorbent [44].

The intraparticle-diffusion model represents a single-resistance model that assumes that the external resistance to mass transfer (film diffusion) is not significant (resulting in no intercept, $C = 0$), or it is significant for a very short period at the beginning of diffusion, where the intraparticle diffusivity (K_d) is constant and does not change with the time [45]. From the graph presented in Figure 3b, it can be seen that the dependence q_t vs. $t^{1/2}$ is not linear and that there are three steps, as previously described. This indicates that the boundary layer diffusion is dominant at the beginning of the sorption, approximately during the first 5 min of the initial DO uptake, where the constant "C" is equal to 4.8909 (Table S2), suggesting that at the beginning of the sorption process, film diffusion is significant; after this period of time, the sorption rate becomes controlled by the intraparticle-diffusion in the next 60 min. Finally, when the PmS-B surface becomes loaded with the DO, the sorption system enters the equilibrium very fast. The obtained trend confirmed the multistep sorption mechanism due to the surface morphology and various functional groups, as described by SEM and FTIR analysis.

3.3. Isotherm Results

Sorption isotherms describe the relationship between the amount of sorbate (that is bonded on the solid surface) and its equilibrium concentration in the fluid phase. The isotherm experiment results are presented in Figure 4, along with fitting curves of applied isotherm models.
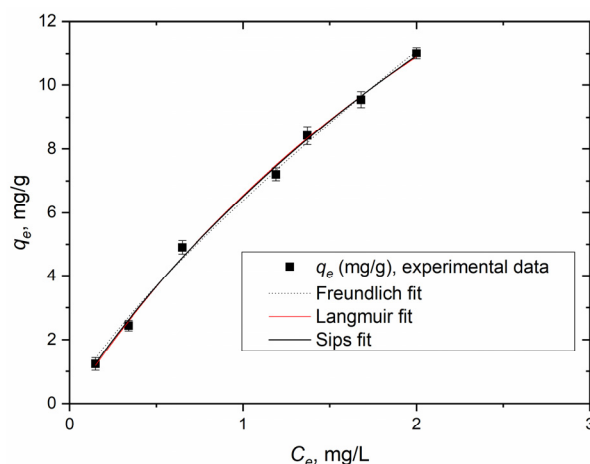

Figure 4. Isotherm model fitting of WSF sorption onto PmS-B.

As can be seen from this graph, the shape of the q_e-C_e curve dependency most probably refers to the Type II isotherm, which is the most typical for non-porous or macroporous materials, where unrestricted monolayer-multilayer sorption might occur [46]. In the case of diesel sorption onto PmS-B, we assume the occurrence of the inflexion point at C_e close to 1 mg/L, which might indicate the stage where the monolayer is fulfilled and the multilayer sorption starts to occur.

In this paper, sorption isotherm experimental results were modelled using non-linear forms of three common isotherm types: Langmuir, Freundlich and Sips (Table S1). The correlation coefficient (R^2) and chi-squared values (χ^2) were used as criteria to determine the best suitable isotherm equation that can be used to describe the DO sorption onto the PmS-B sorbent. The results of the model parameters along with statistical indicators are given in Table S2. As can be seen from the results, the Freundlich model resulted in better fitting of the experimental data with higher R^2 (0.9912) and lower χ^2 (0.0636) values than those of the Langmuir model (0.9841 and 0.0818, respectively). This indicates that the PmS-B surface consists of a variety of sites with different binding energies; the stronger binding sites are occupied first, and the sorption energy is exponentially decreased upon the completion of the sorption process. This is also confirmed by the Freundlich heterogeneity factor ($1/n$), whose value of 0.7943 implies chemisorption [47] as one of the possible mechanisms contributing to overall diesel removal. Isotherm experimental data fitted by the Langmuir isotherm model resulted in the sorption capacity (q_m) of 32.10 mg/g; the value of R_L (calculated as $1/(1 + K_L C_o)$) was found to be in the range from 0.1782 to 0.6612 for the highest and the lowest initial diesel concentrations, respectively, indicating favourable sorption in the investigated concentration range.

However, the data presented in Table S2 indicate that the experimental data obtained for the WSF of DO sorption onto PmS-B are best described by the Sips model—the three-parameter hybrid model of the Langmuir and Freundlich isotherm models. It is well known that the Sips model, at low sorbate concentrations, approaches the Freundlich model, while at higher concentrations, it is closer to the Langmuir model [48]. The surface heterogeneity is described by the Sips model exponent s: a value lower than one indicates a highly heterogeneous system. The value of s was found to be 0.9444, indicating the slightly heterogeneous surface nature of the investigated sorbent. The sorption capacity (q_m), predicted by this model, was found to be 40.72 mg/g, which falls in range with other

sorbents found in the literature applied at a similar initial concentration range [2,5,41]. For example, Barman et al. [41] investigated the sorption of water-soluble PAH fractions of diesel oil-acenaphthene (ACA) and naphthalene (NAP) by biochar made from Indian almond nutshells. Isotherm data, best fitted by Langmuir and Temkin models, indicated that the q_m values were in the range of 18.55–22.18 mg/g and 19.07–22.55 mg/g for ACA and NAP, respectively, suggesting homogeneous, monolayer sorption with strong chemical interaction among biochar and PAH molecules. Comparing sorption properties of toluene onto biochar and commercial activated carbon, Silvani et al. [4] obtained results that also indicated the dual behaviour of the investigated sorbents: isotherm data were well fitted both by the Langmuir model and Freundlich model. Although the specific surface area of the AC was almost two times higher than that of BC, the sorption capacity of BC was higher, which indicated that the occurrence of π–π interactions between hydrophobic organic compounds and the surface of carbonaceous materials play a role in the establishment of stronger sorption interactions.

3.4. Bioremediation

Bioremediation is a technology in which microorganisms transform organic pollutants through reactions that are part of their metabolic processes into less toxic compounds or carbon dioxide and water. The usage of microorganisms as agents for bioremediation is on the rise due to their biodiversity and remarkable catabolic potential. Microorganism's capabilities are conditioned by different adaptation mechanisms, such as modification of cell membranes, production of surface-active substances or usage of an efflux pump to reduce the concentration of toxic components. Some microorganisms have the ability to degrade only a certain number of complex contaminant components, but mixed cultures such as microbial consortiums have a greater degree of degradation. Some of the contaminant's components can only be decomposed co-metabolically—by the joint action of several microorganisms [12]. According to different studies, the species of *Pseudomonas*, *Rhodococcus*, and *Bacillus*, utilized crude oil and its component [49,50]. These microorganisms have been widely used to break down aliphatic hydrocarbons [51].

This part of the study was to investigate the supporting action of bioremediation in the process of purification of water contaminated with diesel (WSF) after achieving a certain degree of removal by plum stone biochar sorption. The purpose of this two-stage process was to reach a certain degree of effluent quality suitable for safe disposal. Both processes support the concept of sustainable development, which is imperative to renewability, efficiency and environmental friendliness.

Gas chromatograms of the three samples are shown in Figure 5. This figure contains three chromatograms related to the starting sample contaminated by diesel (a), the remaining solution after the sorption onto the PmS-B (b) and the solution at the end of the sorption–bioremediation process (c).
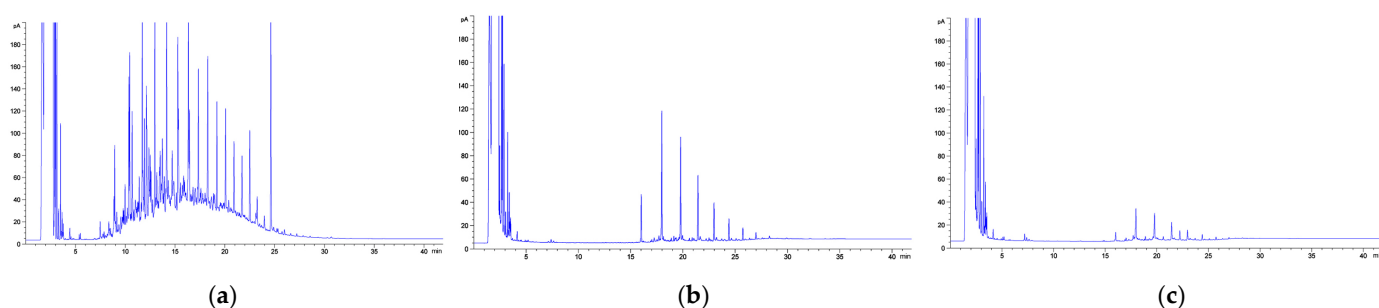

(**a**)　　　　　　　　　　(**b**)　　　　　　　　　　(**c**)

Figure 5. Gas chromatograms of the (**a**) starting solution sample, (**b**) solution sample after the first stage removal and (**c**) final solution sample after the second stage.

Results have shown that most of the DO components are removed by the plum stone biochar sorption, but some portion remains present in the solution (Figure 5b), causing

a potential problem. The application of PmS-B decreased the DO concentration from the initial value of 18 mg/L to the final concentration of 1.71 mg/L. The remaining solution was further subjected to the biodegradation process by microorganisms for 19 days, and the number of HD bacteria was greatly dropped to 10^4 CFU/mL, probably as a consequence of nutrients running out [52]. The concentration of the DO solution was measured and recorded as 0.46 mg/L.

3.5. Eco-Toxicity Tests

The diesel oil application increases the possibility of water pollution due to various accidents throughout the product chain [53]. The negative impact of diesel oil on living organisms indicates the necessity of biological monitoring [53,54]. On the other hand, toxic substances, generated during the pyrolysis that remain in the biochar, might raise a potential environmental risk of biochar application [3]. This is because substances such as organic fractions (VOC, PAHs, dioxins) or heavy metals and persistent free radicals can be leached out from the biochar, causing secondary pollution that can impact plants and microorganisms in water and soil [55]. Keeping this in mind, it is of particular interest to perform some bioassay for an evaluation of the efficiency of the planned remediation process.

An *Aliivibrio fischeri* bioluminescence inhibition bioassay has been widely applied for toxicity monitoring. This test is sensitive, rapid and easy to perform [56]. Eco-toxicity tests were conducted on initial WSF solutions, before (control—C) and after treatment (AT). The results of the acute eco-toxicity test are presented in Figure 6, where different bars represent different dilutions of the starting solutions. The initial WSF concentration was 18 mg/L.
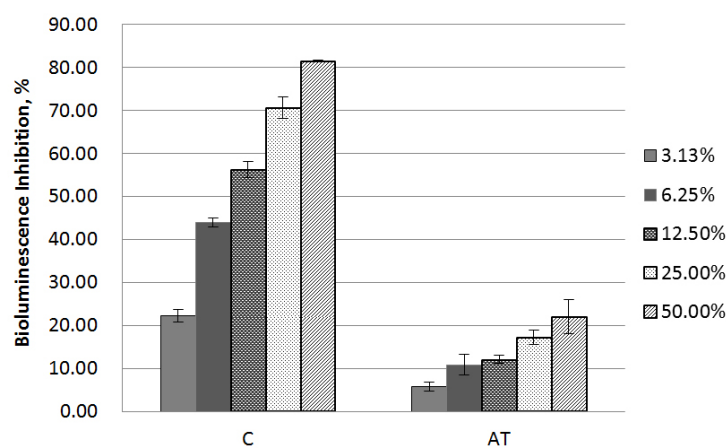

Figure 6. Ecotoxicity of diesel-polluted water before (C) and after treatment (AT).

Diesel-polluted water causes 81.5% of bioluminescence inhibition at the highest tested concentration, with an EC_{50} value of $9.9 \pm 1.7\%$ (1.8 ± 0.03 mg/L). In our previous paper [5], the treatment of polluted water only by the sorption onto peach stone biochar reduced the bioluminescence inhibition from an initial 80% to around 30–40%, regardless of the concentration of the contaminant. Here, the two-stage treatment with PmS-B and microorganisms decreased bioluminescence inhibition to around 5–22%. These results show a significant toxicity decrease after a combined process of sorption and bioremediation treatment.

4. Conclusions

Increased ecological and economic challenges that are rapidly growing worldwide indicate the necessity for the employment of renewable waste materials as valuable resources. Biochar, a stable, solid multipurpose material, has many benefits whose proper applications have the potential to solve these challenges, supporting the principles of the circular economy. Therefore, lignocellulosic waste streams and plum stones were restored from landfills in order to minimize waste disposal, decrease greenhouse gas emissions (by carbon sequestering), and give them a new value.

Pyrolysed waste plum stones were fully characterised and used as an efficient sorbent of WSF—a toxic fraction that is, in most cases, difficult to remove. The obtained results indicate that PmS-B possesses a highly porous surface with plenty of functional groups, increased aromaticity and decreased polarity in comparison to the feedstock, PmS, which is approved by comparing the FTIR spectra of the investigated samples. The elemental organic analysis confirmed that high-quality stabile plum stone biochar with a stronger aromatic structure was obtained after slow pyrolysis. Also, thermo-chemical treatment decreased the polarity of the raw material from the initial value of 0.93 to 0.35, which is in accordance with FTIR analyses. PmS-B has a 50% higher value of pH_{pzc} which indicates an increase in the content of hydroxyl groups, confirmed by FTIR analyses.

The sorption kinetics of the WSF of DO removal follows the pseudo-second-order model, suggesting that the sorption mechanism is limited by bonding forces through electron sharing between the WSF of DO and the PmS-B. Isotherm studies indicated a monolayer–multilayer sorption process, with maximum sorption capacity obtained from the Sips model as 40.72 mg/L, where the diesel sorption might take place primarily by π–π stacking and electrostatic and hydrophobic interactions, which was also confirmed by other researchers. Gas chromatographic analyses showed that after diesel sorption by PmS-B, the initial concentration was reduced by more than 90%, where most of the present aromatic components were removed, but a portion of aliphatic components still remained in the solution. That was the reason for the second treatment phase, bioremediation, after which the total diesel content was reduced by 97.5%. Finally, the toxicity of the purified water sample was tested by applying an *Aliivibrio fischeri* bioluminescence inhibition bioassay. This study also demonstrates that the application of PmS-B sorbent in contaminated water decreases the water toxicity of *Aliivibrio fischeri*, without posing an additional environmental threat.

In conclusion, the described combined process of sorption/bioremediation could be green and cost-effective support for the removal of diesel oil compounds from contaminated waters, with high efficiency and environmental friendliness.

References

1. Xu, Y.; Lu, M. Bioremediation of Crude Oil-Contaminated Soil: Comparison of Different Biostimulation and Bioaugmentation Treatments. *J. Hazard. Mater.* **2010**, *183*, 395–401. [CrossRef]
2. Cai, L.; Zhang, Y.; Zhou, Y.; Zhang, X.; Ji, L.; Song, W.; Zhang, H.; Liu, J. Effective Adsorption of Diesel Oil by Crab-Shell-Derived Biochar Nanomaterials. *Materials* **2019**, *12*, 236. [CrossRef] [PubMed]
3. Wei, Z.; Wei, Y.; Liu, Y.; Niu, S.; Xu, Y.; Park, J.H.; Wang, J.J. Biochar-Based Materials as Remediation Strategy in Petroleum Hydrocarbon-Contaminated Soil and Water: Performances, Mechanisms, and Environmental Impact. *J. Environ. Sci.* **2024**, *138*, 350–372. [CrossRef] [PubMed]
4. Silvani, L.; Vrchotova, B.; Kastanek, P.; Demnerova, K.; Pettiti, I.; Papini, M.P. Characterizing Biochar as Alternative Sorbent for Oil Spill Remediation. *Sci. Rep.* **2017**, *7*, srep43912. [CrossRef] [PubMed]
5. Lopičić, Z.; Avdalović, J.; Milojković, J.; Antanasković, A.; Lješević, M.; Lugonja, N.; Šoštarić, T. Removal of Diesel Pollution by Biochar—Support in Water Remediation. *Hem. Ind.* **2021**, *75*, 329–339. [CrossRef]
6. Santos, C.M.; Dweck, J.; Viotto, R.S.; Rosa, A.H.; de Morais, L.C. Application of Orange Peel Waste in the Production of Solid Biofuels and Biosorbents. *Bioresour. Technol.* **2015**, *196*, 469–479. [CrossRef] [PubMed]
7. Adeleye, A.T.; Akande, A.A.; Odoh, C.K.; Philip, M.; Fidelis, T.T.; Amos, P.I.; Banjoko, O.O. Efficient Synthesis of Bio-Based Activated Carbon (AC) for Catalytic Systems: A Green and Sustainable Approach. *J. Ind. Eng. Chem.* **2021**, *96*, 59–75. [CrossRef]
8. Cha, J.S.; Park, S.H.; Jung, S.C.; Ryu, C.; Jeon, J.K.; Shin, M.C.; Park, Y.K. Production and Utilization of Biochar: A Review. *J. Ind. Eng. Chem.* **2016**, *40*, 1–15. [CrossRef]
9. Kumar, A.; Bhattacharya, T. Biochar: A Sustainable Solution. *Environ. Dev. Sustain.* **2021**, *23*, 6642–6680. [CrossRef]
10. Lopičić, Z.; Antanasković, A.; Šoštarić, T.; Adamović, V.; Orlić, M.; Milojković, J.; Milivojević, M. Improvement of Energy Properties of Lignocellulosic Waste by Thermochemical Conversion into Biochar. *Hem. Ind.* **2023**, *77*, 147–153. [CrossRef]
11. Urgel, J.J.D.T.; Briones, J.M.A.; Diaz, E.B.; Dimaculangan, K.M.N.; Rangel, K.L.; Lopez, E.C.R. Removal of Diesel Oil from Water Using Biochar Derived from Waste Banana Peels as Adsorbent. *Carbon Res.* **2024**, *3*, 13. [CrossRef]
12. Beškoski, V.P.; Gojgić-Cvijović, G.D.; Milić, J.S.; Ilić, M.V.; Miletić, S.B.; Jovančićević, B.S.; Vrvić, M.M. Bioremediation of Soil Polluted with Crude Oil and Its Derivatives: Microorganisms, Degradation, Pathways, Technologies. *Hem. Ind.* **2012**, *66*, 275–289. [CrossRef]
13. Sayara, T.; Sánchez, A. Bioremediation of PAH-Contaminated Soils: Process Enhancement through Composting/Compost. *Appl. Sci.* **2020**, *10*, 3684. [CrossRef]
14. Statistical Office of the Republic of Serbia. Available online: https://data.stat.gov.rs/ (accessed on 16 January 2024).
15. Aurtherson, P.B.; Nalla, B.T.; Srinivasan, K.; Mehar, K.; Devarajan, Y. Biofuel Production from Novel Prunus Domestica Kernel Oil: Process Optimization Technique. *Biomass Convers. Biorefin.* **2023**, *13*, 6249–6255. [CrossRef]
16. Gil, A. Current insights into lignocellulose related waste valorization. *Chem. Eng. J. Adv.* **2021**, *8*, 100186. [CrossRef]
17. *ASTM D 6851-02*; Standard Test Method for Determination of Contact pH with Activated Carbon. ASTM International: West Conshohocken, PA, USA, 2020.
18. Milonjić, S.K.; Ruvarac, A.L.; Sušić, M.V. The Heat of Immersion of Natural Magnetite in Aqueous Solutions. *Termochimica Acta* **1975**, *11*, 261–266. [CrossRef]
19. *ISO 9377-2*; International Standard: Water Quality—Determination of Hydrocarbon Oil Index—Part 2: Method Using Solvent Extraction and Gas Chromatography. International Organization for Standardization: Geneva, Switzerland, 2000.
20. Lukić, M.; Avdalović, J.; Gojgić-Cvijović, G.; Žerađanin, A.; Mrazovac Kurilić, S.; Ilić, M.; Miletić, S.; Vrvić, M.M.; Beškoski, V. Industrial-Scale Bioremediation of a Hydrocarbon-Contaminated Aquifer's Sediment at the Location of a Heating Plant, Belgrade, Serbia. *Clean Technol. Environ. Policy* **2024**, 1–14. [CrossRef]
21. Löser, C.; Seidel, H.; Zehnsdorf, A.; Stottmeister, U. Microbial Degradation of Hydrocarbons in Soil during Aerobic/Anaerobic Changes and under Purely Aerobic Conditions. *Appl. Microbiol. Biotechnol.* **1998**, *49*, 631–636. [CrossRef]
22. Li, X.; Huang, Y.; Liang, X.; Huang, L.; Wei, L.; Zheng, X.; Albert, H.A.; Huang, Q.; Liu, Z.; Li, Z. Characterization of Biochars from Woody Agricultural Wastes and Sorption Behavior Comparison of Cadmium and Atrazine. *Biochar* **2022**, *4*, 27. [CrossRef]
23. Jayakumar, M.; Hamda, A.S.; Abo, L.D.; Daba, B.J.; Venkatesa Prabhu, S.; Rangaraju, M.; Jabesa, A.; Periyasamy, S.; Suresh, S.; Baskar, G. Comprehensive Review on Lignocellulosic Biomass Derived Biochar Production, Characterization, Utilization and Applications. *Chemosphere* **2023**, *345*, 140515. [CrossRef]
24. Tong, Y.; McNamara, P.J.; Mayer, B.K. Adsorption of Organic Micropollutants onto Biochar: A Review of Relevant Kinetics, Mechanisms and Equilibrium. *Environ. Sci. Water Res. Technol.* **2019**, *5*, 821–838. [CrossRef]
25. Yang, M.; Wang, J.; Chen, Y.; Gao, J. Biochar Produced from Cotton Husks and Its Application for the Adsorption of Oil Products. *IOP Conf. Ser. Earth Environ. Sci.* **2020**, *545*, 012022. [CrossRef]
26. Kang, S.; Xing, B. Phenanthrene Sorption to Sequentially Extracted Soil Humic Acids and Humins. *Environ. Sci. Technol.* **2005**, *39*, 134–140. [CrossRef] [PubMed]
27. Chen, B.; Zhou, D.; Zhu, L. Transitional Adsorption and Partition of Nonpolar and Polar Aromatic Contaminants by Biochars of Pine Needles with Different Pyrolytic Temperatures. *Environ. Sci. Technol.* **2008**, *42*, 5137–5143. [CrossRef] [PubMed]
28. Chan, K.Y.; Van Zwieten, L.; Meszaros, I.; Downie, A.; Joseph, S. Agronomic Values of Greenwaste Biochar as a Soil Amendment. *Aust. J. Soil Res.* **2007**, *45*, 629–634. [CrossRef]

29. Katnić, Đ.; Porobić, S.J.; Lazarević-Pašti, T.; Kojić, M.; Tasić, T.; Marinović-Cincović, M.; Živojinović, D. Sterilized Plum Pomace Biochar as a Low-Cost Effective Sorbent of Environmental Contaminants. *J. Water Process Eng.* **2023**, *56*, 104487. [CrossRef]

30. Edeh, I.G.; Masek, O.; Fusseis, F. 4D Structural Changes and Pore Network Model of Biomass during Pyrolysis. *Sci. Rep.* **2023**, *13*, 22863. [CrossRef]

31. Antanasković, A.; Lopičić, Z.; Pehlivan, E.; Adamović, V.; Šoštarić, T.; Milojković, J.; Milivojević, M. Thermochemical Conversion of Non-Edible Fruit Waste for Dye Removal from Wastewater. *Biomass Convers. Biorefin.* **2023**, 1–17. [CrossRef]

32. Šoštarić, T.; Petrović, M.; Stojanović, J.; Marković, M.; Avdalović, J.; Hosseini-Bandegharaei, A.; Lopičić, Z. Structural Changes of Waste Biomass Induced by Alkaline Treatment: The Effect on Crystallinity and Thermal Properties. *Biomass Convers. Biorefin.* **2022**, *12*, 2377–2387. [CrossRef]

33. Stanković, S.; Šoštarić, T.; Bugarčić, M.; Janićijević, A.; Pantović-Spajić, K.; Lopičić, Z. Adsorption of Cu(II) Ions from Synthetic Solution by Sunflower Seed Husks. *Acta Period. Technol.* **2019**, *50*, 268–277. [CrossRef]

34. Šoštarić, T.; Simić, M.; Lopičić, Z.; Zlatanović, S.; Pastor, F.; Antanasković, A.; Gorjanović, S. Food Waste (Beetroot and Apple Pomace) as Sorbent for Lead from Aqueous Solutions—Alternative to Landfill Disposal. *Processes* **2023**, *11*, 1343. [CrossRef]

35. Pehlivan, E.; Altun, T.; Cetin, S.; Iqbal Bhanger, M. Lead Sorption by Waste Biomass of Hazelnut and Almond Shell. *J. Hazard. Mater.* **2009**, *167*, 1203–1208. [CrossRef] [PubMed]

36. Yang, H.; Yan, R.; Chen, H.; Lee, D.H.; Zheng, C. Characteristics of Hemicellulose, Cellulose and Lignin Pyrolysis. *Fuel* **2007**, *86*, 1781–1788. [CrossRef]

37. Yin, C.; Yan, H.; Cao, Y.; Gao, H. Enhanced Bioremediation Performance of Diesel-Contaminated Soil by Immobilized Composite Fungi on Rice Husk Biochar. *Environ. Res.* **2023**, *226*, 115663. [CrossRef]

38. Lehmann, J.; Rillig, M.C.; Thies, J.; Masiello, C.A.; Hockaday, W.C.; Crowley, D. Biochar Effects on Soil Biota—A Review. *Soil Biol. Biochem.* **2011**, *43*, 1812–1836. [CrossRef]

39. Ho, Y.S.; Mckay, G.; Hong, T.; Bay, W.; Kong, H.; Hong, T. Separation & Purification Reviews Kinetics of Pollutant Sorption by Biosorbents: Review. *Sep. Purif. Rev.* **2000**, *29*, 189–232.

40. Blázquez, G.; Martín-Lara, M.A.; Tenorio, G.; Calero, M. Batch Biosorption of Lead(II) from Aqueous Solutions by Olive Tree Pruning Waste: Equilibrium, Kinetics and Thermodynamic Study. *Chem. Eng. J.* **2011**, *168*, 170–177. [CrossRef]

41. Barman, S.R.; Das, P.; Mukhopadhayay, A. Biochar from Waste Sterculia Foetida and Its Application as Adsorbent for the Treatment of PAH Compounds: Batch and Optimization. *Fuel* **2021**, *306*, 121623. [CrossRef]

42. Ho, Y.S.; McKay, G. Pseudo-Second Order Model for Sorption Processes. *Process Biochem.* **1999**, *34*, 451–465. [CrossRef]

43. Simonin, J.P. On the Comparison of Pseudo-First Order and Pseudo-Second Order Rate Laws in the Modeling of Adsorption Kinetics. *Chem. Eng. J.* **2016**, *300*, 254–263. [CrossRef]

44. Koumanova, B.; Peeva, P.; Allen, S.J. Variation of Intaparticle Diffusion Parameter during Adsorption of P-Cholorophenol onto Activated Carbon Made from Apricot Stones. *J. Chem. Technol. Biotechnol.* **2003**, *78*, 582–587. [CrossRef]

45. Malash, G.F.; El-Khaiary, M.I. Piecewise Linear Regression: A Statistical Method for the Analysis of Experimental Adsorption Data by the Intraparticle-Diffusion Models. *Chem. Eng. J.* **2010**, *163*, 256–263. [CrossRef]

46. Sing, K.S.W.; Everett, D.H.; Haul, R.A.W.; Moscou, L.; Pierotti, R.A.; Rouquerol, J.; Siemieniewska, T. Reporting Physisorption Data for Gas/Solid Systems with Special Reference to the Determination of Surface Area and Porosity. *Pure Appl. Chem.* **1985**, *57*, 603–619. [CrossRef]

47. Foo, K.Y.; Hameed, B.H. Insights into the Modeling of Adsorption Isotherm Systems. *Chem. Eng. J.* **2010**, *156*, 2–10. [CrossRef]

48. Witek-Krowiak, A.; Szafran, R.G.; Modelski, S. Biosorption of Heavy Metals from Aqueous Solutions onto Peanut Shell as a Low-Cost Biosorbent. *Desalination* **2011**, *265*, 126–134. [CrossRef]

49. Okoh, E.; Yelebe, Z.R.; Oruabena, B.; Nelson, E.S.; Indiamaowei, O.P. Clean-up of Crude Oil-Contaminated Soils: Bioremediation Option. *Int. J. Environ. Sci. Technol.* **2020**, *17*, 1185–1198. [CrossRef]

50. Rejiniemon, T.S.; R, L.; Alodaini, H.A.; Hatamleh, A.A.; Sathya, R.; Kuppusamy, P.; Al-Dosary, M.A.; Kalaiyarasi, M. Biodegradation of Naphthalene by Biocatalysts Isolated from the Contaminated Environment under Optimal Conditions. *Chemosphere* **2022**, *305*, 135274. [CrossRef] [PubMed]

51. Chaudhary, D.K.; Bajagain, R.; Jeong, S.W.; Kim, J. Biodegradation of Diesel Oil and N-Alkanes (C18, C20, and C22) by a Novel Strain Acinetobacter Sp. K-6 in Unsaturated Soil. *Environ. Eng. Res.* **2020**, *25*, 290–298. [CrossRef]

52. Avdalovic, J.; Duric, A.; Miletic, S.; Ilic, M.; Milic, J.; Vrvic, M.M. Treatment of a Mud Pit by Bioremediation. *Waste Manag. Res.* **2016**, *34*, 734–739. [CrossRef] [PubMed]

53. Müller, J.B.; Melegari, S.P.; Perreault, F.; Matias, W.G. Comparative Assessment of Acute and Chronic Ecotoxicity of Water Soluble Fractions of Diesel and Biodiesel on Daphnia Magna and Aliivibrio Fischeri. *Chemosphere* **2019**, *221*, 640–646. [CrossRef]

54. Hawrot-Paw, M.; Koniuszy, A.; Zając, G.; Szyszlak-Bargłowicz, J. Ecotoxicity of Soil Contaminated with Diesel Fuel and Biodiesel. *Sci. Rep.* **2020**, *10*, 16436. [CrossRef]

55. Zhang, Y.; Yang, R.; Si, X.; Duan, X.; Quan, X. The Adverse Effect of Biochar to Aquatic Algae- the Role of Free Radicals. *Environ. Pollut.* **2019**, *248*, 429–437. [CrossRef] [PubMed]

56. Abbas, M.; Adil, M.; Ehtisham-ul-Haque, S.; Munir, B.; Yameen, M.; Ghaffar, A.; Shar, G.A.; Asif Tahir, M.; Iqbal, M. Vibrio Fischeri Bioluminescence Inhibition Assay for Ecotoxicity Assessment: A Review. *Sci. Total Environ.* **2018**, *626*, 1295–1309. [CrossRef] [PubMed]

57. Lagergren, S. About the Theory of so Called Adsorption of Soluble Substances. *K. Sven. Vetenskapsakademiens Handl.* **1898**, *24*, 1–39.
58. Chien, S.H.; Clayton, W. Application of Elovich Equation to the Kinetics of Phosphate Release and Sorption in Soils. *Soil Sci. Soc. Am. J.* **1980**, *44*, 265–268. [CrossRef]
59. Weber, W.J.; Morris, J.C. Kinetics of Adsorption on Carbon from Solution. *J. Sanit. Eng. Div.* **1963**, *89*, 31–60. [CrossRef]
60. Langmuir, I. The Adsorption of Gases on Plane Surfaces of Glass, Mica and Platinum. *Am. Chem. Soc.* **1918**, *40*, 1361–1403. [CrossRef]
61. Freundlich, H.M.F. Over the Adsorption in Solution. *J. Phys. Chem.* **1906**, *57*, 385–470.
62. Sips, R. Combined Form of Langmuir and Freundlich Equations. *J. Chem. Phys.* **1948**, *16*, 490–495. [CrossRef]